



Thota, P., Krauskopf, B., & Lowenberg, MH. (2008). *Shimmy in a nonlinear model of an aircraft nose landing gear with non-zero rake angle*. <http://hdl.handle.net/1983/1060>

Early version, also known as pre-print

[Link to publication record in Explore Bristol Research](#)  
PDF-document

## University of Bristol - Explore Bristol Research

### General rights

This document is made available in accordance with publisher policies. Please cite only the published version using the reference above. Full terms of use are available:  
<http://www.bristol.ac.uk/red/research-policy/pure/user-guides/ebr-terms/>

# SHIMMY IN A NONLINEAR MODEL OF AN AIRCRAFT NOSE LANDING GEAR WITH NON-ZERO RAKE ANGLE

Phanikrishna Thota\*, Bernd Krauskopf\* and Mark Lowenberg\*\*

\*Dept of Engineering Mathematics, \*\*Dept of Aerospace Engineering  
University of Bristol, BS8 1TR, UK.

## Abstract

This work concentrates on the lateral oscillations in vehicles, also called shimmy, with a particular emphasis on aircraft. A mathematical model of a nose landing gear is discussed with geometric detail that has been mostly neglected in the past research. Stability criteria for the shimmy-free operation of the landing gear are derived using linear stability analysis. Nonlinear analysis is used not only to study the qualitative behaviour of the Hopf bifurcation but also to analyze the system beyond the Hopf bifurcation. The manuscript concludes with suggestions for future research.

## 1 Introduction

Wheeled vehicles, including automobiles, pulled trailers, motorcycles, and aircraft, occasionally experience self-excited, lateral oscillations due to a variety of flexibilities involved in their design. This phenomenon, conventionally referred to as *shimmy*, results in wearing of the related mechanical components and, hence, is undesirable in the operation of the vehicle. In an aircraft, dealing with shimmy may incur heavy maintenance costs. In extreme cases, the induced vibration can be so violent as to limit the pilot's ability to see and read the instrument panel. Yet, the onset of shimmy in aircraft is far from fully understood, which provides the motivation for this work.

A landing gear mainly consists of a strut attached to the fuselage of the aircraft that includes oleos (dampers), torque-links, steering mechanism, etc. The strut is coupled to the ground via one or more wheels with flexible tyres mounted on an axle. Figure 1 shows schematic side, back and top views of a nose landing gear. Here, the strut, which is inclined to the vertical at a *rake angle*  $\phi$ , rotates about its axis with a *steering angle*  $\psi$ . The strut is connected to the wheel's axle with a mechanical trail (*caster*) of length  $e$ . The presence of the non-zero rake angle  $\phi$  in the landing gear induces an effective caster length  $e_{\text{eff}}$ , as well as a tilt  $\gamma$  of the wheel(s) for non-zero steering angle  $\psi$ . Furthermore, the *swivel angle*  $\theta$  of the wheel with the ground is different from the steering angle  $\psi$ ; see Sec. 3 for details.

Note that we are using throughout one of the conventionally accepted coordinate systems for aircraft analysis. Specifically, the positive  $x$ -axis points towards the backward direction of the aircraft, the  $z$ -axis is the upward normal to the (flat) ground, and the  $y$ -axis completes the right-handed coordinate system.

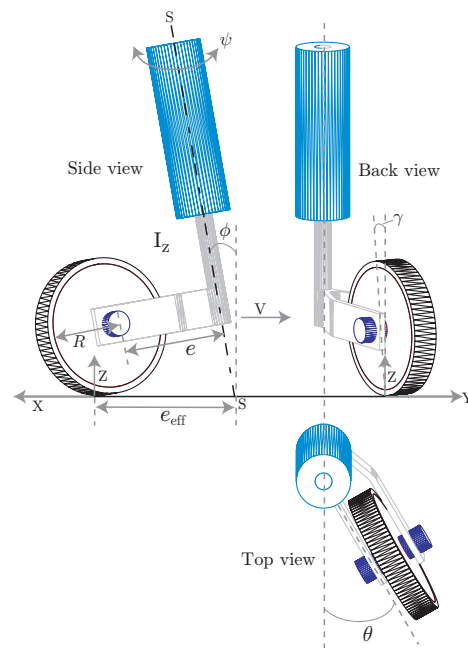


Figure 1. Schematic of a nose landing gear of an aircraft.

The structure shown in Fig. 1 closely resembles the landing gear of an aircraft, which is characterized by a moderate rake angle (about  $10^\circ$ ), a small caster length (about 0.1 m for a mid-size passenger aircraft), and large torsional stiffness and damping due to the hydraulic steering mechanism. For comparison, motorcycles generally have large rake angles (possibly even larger than  $30^\circ$ ) and a small caster length, while trailers have zero rake angle and a long caster length (up to several metres). Importantly, both motorcycles and trailers generally have very low torsional damping.

The overall model consists of both the geometry of the vehicle and a choice of tyre model. We consider here an aircraft landing gear, characterized by typical values of the parameters as discussed above. In particular, we consider a model that includes geometric effects of a non-zero rake angle. While the rake angle of a typical aircraft landing gear is indeed non-zero, no previous study of shimmy in aircraft has taken proper consideration of a non-zero rake angle. In fact, most authors set the rake angle to zero; see also Section 2. The wheel-ground interaction is modelled by the well-established stretched string model from [von Schlippe and Dietrich, 1947] of an elastic tyre. Throughout we use realistic parameters for geometry and tyre modelling taken from [Somieski, 1997] and summarized in Table 1. The vertical force  $F_z$  on the gear and the forward velocity  $V$  of the aircraft are identified as two key parameters influencing the stability of the gear. They are used as free parameters in this study.

From a dynamical systems point of view, the onset of shimmy oscillations is via the transition through a Hopf bifurcation when a parameter is changed. This leads to the onset of periodic lateral motion of the wheel. In this paper we study the Hopf bifurcation in dependence on the vertical force  $F_z$  and the velocity  $V$  to identify the region where shimmy oscillations may occur. We also discuss the criticality of the Hopf bifurcation as a means of determining the stability of the bifurcating oscillations. This information is important for determining whether the landing gear is operationally safe.

This paper is organized as follows. Section 2 gives a brief review of the literature on shimmy with particular emphasis on aircraft. Details of the mathematical model of a nose landing gear are introduced in Sec. 3. Linear stability analysis of the mathematical model is discussed in Sec. 4, as is its nonlinear dynamics in Sec. 5. Finally, Sec. 6 summarizes the work with suggestions for future research.

## 2 Brief discussion of the literature

We briefly describe some important works in the area of shimmy analysis in vehicle dynamics with particular relevance to aircraft; further reading can be found in the survey papers [Dengler *et al.*, 1951; Smiley, 1957; Pritchard, 1999].

Even though elastic tyres have been in use for over a century, modeling a rolling tyre still remains one of the most difficult problems in the area of vehicle dynamics. Particularly, the complications that arise in the tyre-ground contact area along with the nonlinear elastic nature of the rubber make the modeling process difficult. Broulhiet, in 1925, published his seminal work on the effect of tyre mechanics on shimmy [Broulhiet, 1925]. The principles stated in his work still form the basis in studying these self-excited oscillations [Dengler *et al.*, 1951]. Broulhiet first described the concept of *side-slip* and suggested that the energy for the self-sustenance of the shimmy oscillations comes from the tyre mechan-

ics via the side-slip. A number of tyre theories were reported in the last half a century, but only a few of them have been found to be consistent with the experimental data, notable examples are [Moreland, 1925], [Pacejka, 1965; Pacejka, 1966] and [von Schlippe and Dietrich, 1947]. In the model in Sec. 3 we use the stretched string model of [von Schlippe and Dietrich, 1947], which is widely accepted as a successful model of the kinematics of an elastic tyre.

Several researchers studied the shimmy phenomenon in aircraft using experimental, analytical and numerical techniques [Baumann, 1995; Besselink, 2000; Glaser and Hrycko, 1995; Krabacher, 1995; Smiley, 1957]. Apart from correlating different tyre theories, [Smiley, 1957] studied shimmy for three different cases of landing gear structures. While one of the cases has a non-zero rake angle, its nonlinear geometric effects were not included in the model. The paper [Smiley, 1957] contains a stability analysis and discusses a systematic way of modeling the geometrical aspects of the strut in an aircraft landing gear. More recently, [Somieski, 1997] studied shimmy as a nonlinear dynamics phenomenon for a nonlinear set of ODEs describing a nose landing gear with zero rake angle. Here, time domain analysis showed a case of *supercritical* Hopf bifurcation leading to a set of stable limit cycles past the bifurcation point. In fact, for simplicity of the models almost all past research on aircraft shimmy was performed for a zero rake angle. This means that geometrical and, hence, nonlinear aspects of a nonzero rake angle have not been taken into account.

Shimmy has also been studied in a general wheeled vehicle setting. We mention here a number of references that use nonlinear dynamics methods, which mostly concern the case of a pulled trailer. Pacejka [Pacejka, 1966] studied shimmy in the presence of friction and freeplay in the kingpin. [Stépán, 1991] studied shimmy for a trailer configuration with zero torsional damping at the rotation axis and with zero rake angle for both rigid and elastic tyres. He showed that the Hopf bifurcation responsible for the onset of oscillations is subcritical in this case, so that the system may suddenly jump to large amplitude oscillations. A stability criterion in terms of the caster length was derived in [Stépán, 1998]. The transition from sub- to supercritical Hopf bifurcation as the lateral damping is increased was found in [Takacs *et al.*, 2007] to involve a saddle-node Hopf bifurcation.

## 3 Mathematical model

Consider the landing gear assembly shown in Fig. 1. Here, the combined mass of the aircraft's fuselage and wings is assumed to be a single lumped mass that exerts a vertical force  $F_z$  on the gear. According to von Schlippe's stretched string model, the kinematic relationship between the swivel angle  $\theta$  and the lateral deformation  $\lambda$  of the leading edge of the contact patch is

given by

$$\dot{\lambda} + \frac{V}{L}\lambda = V\theta + (e_{\text{eff}} - h)\dot{\theta}. \quad (1)$$

Our model considers moments due to the stiffness and damping of the strut, and a damping force due to tyre tread width. Using Newton's second law, the equations for the landing gear model considered here are given by [Somieski, 1997] as

$$Iz\ddot{\psi} = M_{F_1}(\psi) + M_{D_1}(\dot{\psi}) + M_2(\lambda) + M_{D_\lambda}(\dot{\theta}). \quad (2)$$

Here the moment  $M_{F_1}$  due to the torsional stiffness of the strut is given by

$$M_{F_1}(\psi) = c\psi, \quad (3)$$

and the moment  $M_{D_1}$  due to the torsional damping of the strut is given by

$$M_{D_1}(\dot{\psi}) = k_1\dot{\psi}. \quad (4)$$

The last two terms in Eq. (2) model the tyre interaction with the ground. Specifically, the combined moment  $M_2$  due to the tyre's restoring force  $F_{t_\lambda}$  and self-aligning moment  $M_{t_\alpha}$ , is given by

$$M_2(\lambda) = M_{t_\alpha} - e_{\text{eff}}F_{t_\lambda}, \quad (5)$$

where

$$M_{t_\alpha} = \begin{cases} \frac{F_z C_{M_\alpha}}{18} \sin(18\alpha) & \text{if } |\alpha| \leq \alpha_g, \\ 0 & \text{if } |\alpha| > \alpha_g, \end{cases} \quad (6)$$

and

$$F_{t_\lambda} = \begin{cases} C_{F_\alpha} F_z \alpha & \text{if } |\alpha| \leq \delta, \\ C_{F_\alpha} F_z \delta \text{sign}(\alpha) & \text{if } |\alpha| > \delta. \end{cases} \quad (7)$$

Finally, the moment  $M_{D_\lambda}$  due to the tyre's tread width damping is given by

$$M_{D_\lambda}(\dot{\theta}) = \frac{k_2}{V}\dot{\theta}. \quad (8)$$

The slip angle  $\alpha$  is related to the lateral deformation  $\lambda$  by  $\alpha = \tan^{-1}(\frac{\lambda}{L})$ . The rake angle  $\phi$  enters into our model via the effective caster length

$$e_{\text{eff}} = e \cos \phi + R \tan \phi + e \sin \phi \tan \phi, \quad (9)$$

where  $R$  is the radius of the tyre; note that  $e_{\text{eff}} = e$  for  $\phi = 0$ . Here,  $e_{\text{eff}} = 0.1788$  m for parameters in Table

1, which is about 50% increase in  $e$  for  $\phi \neq 0$ . Furthermore,  $\phi$  induces the geometrical relation  $\theta = \psi \cos(\phi)$  between the steering angle  $\psi$  and the swivel angle  $\theta$ . Finally,  $\phi \neq 0$  implies that steering results in a tilt angle  $\gamma \neq 0$  of the tyre, but this effect is not taken into account in the tyre model considered here. In the above equations,  $c$ ,  $k_1$ ,  $k_2$ ,  $C_{M_\alpha}$  and  $C_{F_\alpha}$  are experimentally measured constants as detailed in Table 1.

#### 4 Linear stability analysis

The linearization of Eqs. (1) and (2) w.r.t. the state vector  $\mathbf{x} = (\psi, \dot{\psi}, \lambda)^T$  is given by the Jacobian matrix

$$D\mathbf{f}(\mathbf{0}) = \begin{pmatrix} 0 & 1 & 0 \\ c_1 & c_2 & c_3 \\ V & c_4 & c_5 \end{pmatrix}, \quad (10)$$

where

$$c_1 = \frac{c}{I_z}, \quad (11)$$

$$c_2 = \frac{k_1}{I_z} + \frac{k_2}{V I_z}, \quad (12)$$

$$c_3 = \frac{(C_{M_\alpha} - e_{\text{eff}} C_{F_\alpha}) F_z}{I_z L}, \quad (13)$$

$$c_4 = e_{\text{eff}} - h, \quad (14)$$

$$c_5 = \frac{-V}{L}. \quad (15)$$

Hence, stability is determined by the characteristic equation

$$s^3 - (c_2 + c_5)s^2 + (c_2c_5 - c_1 - c_3c_4)s + (c_1c_5 - Vc_3) = 0. \quad (16)$$

With the Routh-Hurwitz stability criterion it can be concluded from Eq. (16) that the linearized system is stable if

$$c_2 + c_5 < 0, \quad (17)$$

$$c_2c_5 - c_1 - c_3c_4 > 0, \quad (18)$$

$$c_1c_5 - Vc_3 > 0, \quad (19)$$

$$[(c_1c_5 - Vc_3) + (c_2c_5 - c_1 - c_3c_4)(c_2 + c_5)] < 0. \quad (20)$$

With the definitions (11)–(15) of the constants  $c_1 \dots c_5$  the above stability criteria are complicated algebraic expressions when expressed in all generality in all parameters. Hence, a parameter dependent linear stability analysis, even for realistic sub-cases of interest for aircraft shimmy, is quite involved and beyond the scope of this paper.

Instead, we consider here the special case where the strut does not exert stiffness and damping and that there

is no damping from the tyre's tread. This means that  $k_1 = 0$ ,  $k_2 = 0$  and  $c = 0$ , so that Eqs. (17)–(19) evaluate to  $\frac{V}{L} > 0$ , which is always satisfied. Therefore, stability is determined exclusively by Eq. (20), which, since  $(C_{M\alpha} - e_{\text{eff}} C_{F\alpha}) < 0$ , reduces to

$$e_{\text{eff}} > h + L. \quad (21)$$

This is exactly the criterion derived in [Stépán, 1998] for  $\phi = 0$  and, hence,  $e_{\text{eff}} = e$ , which says that, in the absence of stiffness and damping in the landing gear and tyre, a minimum caster length is required to avoid shimmy oscillations. While the assumption of zero stiffness and damping is not realistic for an actual aircraft landing gear, it shows that our model reproduces the reported stability property for this case (which is more realistic for a pulled trailer).

More generally, linear stability analysis can assist designers in determining the parameter regions defining stability. Specifically, damping and stiffness characteristics, caster length, and rake angle could be optimised to ensure that the landing gear operates safely away from the stability boundary. However, a nonlinear analysis is also required, for example, to study the properties of ensuing shimmy oscillations and their dependence on parameters.

## 5 Nonlinear dynamics

To analyze the behaviour of Eqs. (1)–(2) beyond the Hopf bifurcation we perform a numerical bifurcation analysis with the software AUTO [Doedel *et al.*, 1991]. Specifically, we follow periodic orbits and the Hopf bifurcation itself in the vertical force  $F_z$  and the forward velocity  $V$ .

For  $F_z$  and  $V$  as given in Table 1 the origin ( $\mathbf{x} = \mathbf{0}$ , which models the tyre rolling in a straight line) is asymptotically stable, meaning that any perturbation decays as  $t$  tends to  $\infty$ . However, the stability of the origin changes when the vertical force  $F_z$  is changed. Specifically, as seen in Fig. 2(a), at  $F_z \approx 9231$  N there is a Hopf bifurcation that results in periodic oscillations for  $F_z$  beyond the bifurcation point. In terms of the landing gear dynamics, the Hopf bifurcation marks the onset of shimmy. It is important to note that the Hopf bifurcation is supercritical, that is, the bifurcating periodic oscillations are asymptotically stable. This implies that a sudden increase of the vertical force  $F_z$ , for example, during the landing phase of an aircraft, may trigger shimmy oscillations. A related effect can be observed in motorcycles: stability may be lost immediately after the front wheel comes down after a manoeuvre such as a jump.

Figure 2(b) shows that the origin also loses its stability under variation of the forward velocity  $V$ . Specifically, at  $V \approx 74.4$  m/s stable oscillations are born in a supercritical Hopf bifurcation. Note that these oscillations disappear again in another supercritical Hopf bifurcation as  $V$  is increased past  $V \approx 155.0$  m/s. The disap-

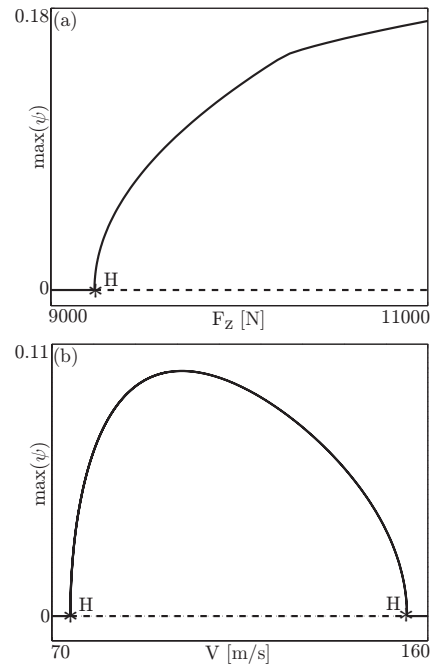


Figure 2. Hopf bifurcation to stable periodic orbits for fixed  $V = 70$  m/s and varying  $F_z$  (a), and for fixed  $F_z = 9000$  N and varying  $V$  (b); solid curves correspond to stable and dashed curves to unstable solutions.

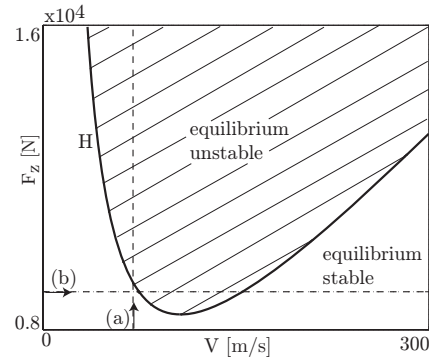


Figure 3. The Hopf bifurcation curve in the  $(V, F_z)$ -plane divides the region of stable operation from the region of shimmy oscillations (shaded); the dashed lines indicate the locations of the one-parameter continuations shown in Fig. 2.

pearance of shimmy with increasing speed has indeed been observed in practice.

Figure 3 shows a two-parameter continuation of the curve of Hopf bifurcation in the  $(V, F_z)$ -plane. It divides this parameter space into two region for which the zero equilibrium is stable and unstable, respectively. For  $F_z < 8405$  N the zero equilibrium is always stable, which means that there are no shimmy oscillations for any value of the velocity  $V$ . For  $F_z > 8405$  N, on the other hand, there exists a range of velocities (in the shaded region) where the zero equilibrium is unstable. Our continuation shows that the Hopf bifurcation is supercritical along the curve  $H$ , so that one observes stable shimmy oscillations near this stability boundary;

cf. Fig. 2(b). Further inside the shaded region the associated stable periodic orbit may undergo further stability changes in a variety of bifurcation scenarios. This would result in more complicated lateral motions of the wheel, which is an interesting topic beyond the scope of this paper.

### 5.1 Hopf bifurcation analysis

We investigated the criticality of the Hopf bifurcation by means of a centre manifold analysis, details of which will appear elsewhere. This analysis suggests that the Hopf bifurcation is supercritical in the range of realistic parameter values that correspond to an aircraft leading gear, which confirms the numerical observation in Fig. 2. By contrast, [Stépán, 1998] and [Takacs *et al.*, 2007] reported (for the case of a trailer) that the Hopf bifurcation is subcritical in the absence of torsional stiffness and damping. We find that our model also displays subcritical Hopf bifurcations for zero torsional stiffness and damping. However, very small amounts of torsional damping already result in a supercritical Hopf bifurcation; this transition is associated with a saddle-node Hopf bifurcation. This agrees with the result in [Takacs *et al.*, 2007] concerning the influence of lateral damping at the kingpin of the trailer.

### 6 Summary and future work

We presented a model for an aircraft nose landing gear that includes geometric effects due to a non-zero rake angle. The Hopf bifurcation that corresponds to the onset of shimmy was continued in the vertical force and the forward velocity of the aircraft. The onset of shimmy oscillations was found to be supercritical for realistic values of the parameters, mainly due to strong torsional damping.

There are several directions for future research. First of all, we plan to assess the influence of other parameters on the onset of shimmy. This study will include operational parameters, for example, the contact patch length  $h$  (which is related to tyre pressure), as well as design parameters of the landing gear itself, such as the caster length and the rake angle. Secondly, we will consider interdependencies between parameters. For example, the contact patch length  $h$  varies with vertical force  $F_z$ , which in turn decreases with an increasing velocity  $V$ . Furthermore, the velocity  $V$  itself is not constant but changes in characteristic ways during taxiing, take-off and landing. Finally, effects that are presently not modelled will be included at a later stage; examples are bending and lateral motion of the strut, and the coupling of the nose landing gear to the other gears via the fuselage.

### 7 Acknowledgments

The authors are grateful to Airbus UK for financial support of this research.

### References

- J. Baumann, A Nonlinear Model for Landing Gear Shimmy with Applications to the McDonnell Douglas G/A-18A, 81<sup>st</sup> Meeting of the AGARD Structures and Materials Panel, 1995.
- I. J. M. Besselink, Shimmy of Aircraft Main Landing Gears, Dissertation, University of Delft, The Netherlands, 2000.
- M. G. Brouhiet, La Suspension de la direction de la voiture automobile - Shimmy et dandinement, Bull. Soc. Ing. Civ.(France), Vol 78, 1925.
- M. Dengler, M. Goland and G. Herrman, A bibliographic survey of automobile and aircraft wheel shimmy, Technical report, Midwest Research Institute, Kansas city, MO, USA, 1951.
- E. J. Doedel, H. B. Keller, and J. P. Kernevez, Numerical analysis and control of bifurcation problems, Part II : Bifurcation in infinite dimensions, J. Bifur. Chaos Appl. Sci. Engrg., 1(4), pp. 745–772, 1991.
- J. Glaser and G. Hrycko, Landing Gear Shimmy - De Havilland's Experience, 81<sup>st</sup> Meeting of the AGARD Structures and Materials Panel, 1995.
- W. E. Krabacher, A Review of Aircraft Landing Gear Dynamics, 81<sup>st</sup> Meeting of the AGARD Structures and Materials Panel, 1995.
- W. J. Moreland, Landing-Gear Vibration, AF Tech. Rep. No. 6590, Wright Air Dev. centre, 1951.
- H. B. Pacejka, Analysis of the shimmy phenomenon, Proceedings of The Institute of Mechanical Engineers, 180(2A)(10), 1965-66.
- H. B. Pacejka, The wheel shimmy phenomenon: A theoretical and experimental investigation with particular reference to the nonlinear problem, Dissertation, Delft University of Technology, 1966.
- I. J. Pritchard, An overview of landing gear dynamics, NASA Technical Reports, NASA/TM-1999-209143, 1999.
- R. F. Smiley, Correlation, evaluation, and extension of linearized theories for tyre motion and wheel shimmy, report submitted to the National Advisory Committee for Aeronautics, Report 1299, 1957.
- G. Somieski, Shimmy analysis of a simple aircraft nose landing gear model using different mathematical methods, Aerospace Science and Technology, 1270-9638 (8), 1997.
- G. Stépán, Delay, Nonlinear Oscillations and Shimmying Wheels, Kluwer Academic Publishers, Dordrecht, 1998.
- G. Stépán, Chaotic motion of wheels, Vehicle System Dynamics, 20(6), pp. 341–351, 1991.
- D. Takacs., G. Stépán, and J. H. Hogan, Isolated Large Amplitude Periodic Motions of Towed Rigid Wheels, Nonlinear Dynamics, April, 2007.
- B. von Schlippe and R. Dietrich, Shimmying of a pneumatic wheel, report submitted to the National Advisory Committee for Aeronautics, NACA TM 1365, 1947.

Table 1. System parameters and their values as used in the modeling.

Parameter	Description	Value
	<i>structure parameters</i>	
$e$	caster length	0.12 m
$c$	torsional stiffness of strut	$-1.0 \times 10^5$ N m rad <sup>-1</sup>
$k_1$	torsional damping of strut	-45.0 N m s rad <sup>-1</sup>
$I_z$	moment of inertia of strut	1.0 kg m <sup>2</sup>
$\phi$	rake angle	0.1571 rad (9°)
	<i>tyre parameters</i>	
$R$	radius of nose wheel	0.362 m
$h$	contact patch length	0.1 m
$k_2$	damping coefficient of elastic tyre	-270.0 N m <sup>2</sup> rad <sup>-1</sup>
$C_{M_\alpha}$	self-aligning coefficient of elastic tyre	-2.0 m/rad
$C_{F_\lambda}$	restoring coefficient of elastic tyre	20.0 rad <sup>-1</sup>
$L$	relaxation length	0.3 m
$\delta$	restoring force limit	0.0873 rad (5°)
$\alpha_g$	self-aligning moment limit	0.1745 rad (10°)
	<i>continuation parameters</i>	
$F_z$	vertical force on the gear	9000 N
$V$	forward velocity	70.0 m s <sup>-1</sup>